AD-A056 367 ARMY ARMAMENT RESEARCH AND DEVELOPMENT COMMAND ABERD--ETC F/G 7/4
SUMMARY OF PHOTODESTRUCTION CROSS SECTION MEASUREMENTS OF ATMOS--ETC(U)
MAY 78 J A VANDERHOFF DAHC04-74-G-0192
UNCLASSIFIED ARBRL-TR-02070 SBIE-AD-E430 066 NL

| OF |
ADA
056367

END
DATE
FILMED
8-78
DDC

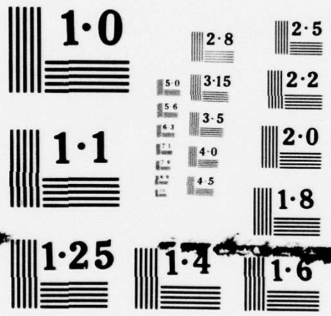

NATIONAL BUREAU OF STANDARDS
MICROCOPY RESOLUTION TEST CHART

UNCLASSIFIED

SECURITY CLASSIFICATION OF THIS PAGE (When Data Entered)

REPORT DOCUMENTATION PAGE

READ INSTRUCTIONS
BEFORE COMPLETING FORM

1. REPORT NUMBER (14) TECHNICAL REPORT ARBRL-TR-02070
2. GOVT ACCESSION NO.
3. RECIPIENT'S CATALOG NUMBER (9)

4. TITLE (and Subtitle) (6)
SUMMARY OF PHOTODESTRUCTION CROSS SECTION MEASUREMENTS OF ATMOSPHERIC IONS,
5. TYPE OF REPORT & PERIOD COVERED
Technical rept.
~~6. PERFORMING ORG. REPORT NUMBER~~

7. AUTHOR(s) (10)
JOHN A./VANDERHOFF
8. CONTRACT OR GRANT NUMBER(s)

9. PERFORMING ORGANIZATION NAME AND ADDRESS
US Army Ballistic Research Laboratory
(ATTN: DRDAR-BLB)
Aberdeen Proving Ground, MD 21005
10. PROGRAM ELEMENT, PROJECT, TASK AREA & WORK UNIT NUMBERS (17)
DNA Subtask (16) S99QAXHD411

11. CONTROLLING OFFICE NAME AND ADDRESS
US Army Armament Research and Development Command
US Army Ballistic Research Laboratory
(ATTN: DRDAR-BL)
Aberdeen Proving Ground, MD 21005
12. REPORT DATE (11)
MAY 1978
May 78
13. NUMBER OF PAGES
40

14. MONITORING AGENCY NAME & ADDRESS (if different from Controlling Office)
15. SECURITY CLASS. (of this report) (12) 34 p.
Unclassified
15a. DECLASSIFICATION/DOWNGRADING SCHEDULE

16. DISTRIBUTION STATEMENT (of this Report)
Approved for public release; distribution unlimited

D D C
RECEIVED
JUL 20 1978
B

17. DISTRIBUTION STATEMENT (of the abstract entered in Block 20, if different from Report)

18. SUPPLEMENTARY NOTES
(18) SBIE (19) AD-E430 066

19. KEY WORDS (Continue on reverse side if necessary and identify by block number)

Photodestruction	Cluster Ions
Photodissociation	Photon-Ion Interaction
Photodetachment	
Atmospheric Ions	

20. ABSTRACT (Continue on reverse side if necessary and identify by block number) (eal)

Using a drift tube mass spectrometer coupled with a laser photon source absolute photodestruction cross sections as a function of photon energy have been measured for various room temperature (300 K) atmospheric ions. These ions are O_2^-, O_3^-, O_4^-, NO_2^-, SO_2^-, $O_2^-(H_2O)$, CO_4^-, SO_4^-, $O_2^+(O_2)$, $O_2^+(H_2O)$, $O_2^-(CO_2)$, $O_2^-(SO_2)$, $CO_2^-(CO_2)$, and $H^+(H_2O)_{n=1-4}$.

sub n=1 to 4

DD FORM 1 JAN 73 1473 EDITION OF 1 NOV 65 IS OBSOLETE

78 06 27 049

UNCLASSIFIED

SECURITY CLASSIFICATION OF THIS PAGE (When Data Entered)

393 471

act

TABLE OF CONTENTS

LIST OF ILLUSTRATIONS

LIST OF TABLES

INTRODUCTION

The ability to predict the performance of radar and radio communications depends upon the density and species of charged particles in the atmosphere. The interaction of light (solar or nuclear burst) with atmospheric ions is an important process which can alter the charged particle species. Photodetachment produces free electrons and photodissociation can change both positive and negative ion species.[1-3] Photodissociation of a complex negative ion into a simpler fragment followed by photodetachment of this fragment is another method of producing free electrons.

These photoprocesses for atmospheric ions have received little investigation and those studies made were typically with broadband light sources.[4-6] With the availability of high intensity tunable laser light it became feasible to make detailed measurements on photodissociation and photodetachment processes. The research reported here is a summary of BRL measurements of photodestruction (photodetachment and/or photodissociation) cross sections of atmospheric ions using tunable laser radiation.

EXPERIMENTAL

Experimental measurements geared to produce photodestruction cross sections applicable to the atmosphere should be performed on ions in the same energy state or states as those found in the atmosphere. Due to the many thermal energy ion-neutral collisions of the ions with the neutral gas the majority of atmospheric ions are thermalized. Thus measurements ideally should be made under field free conditions at a

---

[1] L. Thomas, P. M. Gondhalecar and M. R. Bowman, "Photodetachment of Electrons from Negative Ions in the Lower D Region," Nature 238, 89-90 (1972).

[2] L. Thomas and M. R. Bowman, "A Theoretical Study of Negative Ion Changes in the D Region During an Eclipse," J. Atmos. Terr. Phys. 36, 1411-1420 (1974).

[3] J. R. Peterson, "Sunlight Photodestruction of CO_3^-, $CO_3^- \cdot H_2O$, and O_3^-: The Importance of Photodissociation to the D Region Electron Densities at Sunrise," J. Geophys. Res. 81, 1433-1435 (1976).

[4] L. M. Branscomb, S. J. Smith, and G. Tisone, "Oxygen Metastable Atom Production Through Photodetachment," J. Chem. Phys. 43, 2906-2907 (1965), and references contained therein.

[5] S. P. Hong, S. B. Woo, and E. M. Helmy, "Photodetachment of Thermally Relaxed CO_3^-," Phys. Rev. A 15, 1562-1569 (1977), and references contained therein.

[6] P. Warneck, "Laboratory Measurements of Photodetachment Cross Sections of Selected Negative Ions," GCA Technical Report 69-13-N, GCA Corporation, Bedford, MA (1969).

temperature corresponding to the particular altitude region of atmospheric interest. A drift tube source was chosen to form the ions as this type of source can produce thermalized ions when operated at low field conditions and moderate pressures.

The experiment has been discussed in detail previously[7] hence only a brief description of the apparatus and added features will be presented here. Basically the experiment consists of a drift tube with mass spectrometric analysis and a laser light source. It is shown schematically on Fig. 1. Ion species are created within the drift tube by a hot filament electron impact source and their energy is controlled by a uniform electric field which can be varied. Just prior to exiting the uniform field region, the ion swarm is intersected by a chopped monoenergetic photon beam. The resultant ion beam is then mass analyzed and detected. By correlating this signal with the time the photon beam is on and off, photodestruction cross sections are measured. The amount of photodissociation present in the photodestruction measurements may be determined by observing a creation or increase in simpler (photofragment) ions during the time the photon beam is on.

Three continuous duty laser sources have been used to provide photon flux in the range of 800 to 350 nm. The discrete lines of the argon and krypton ion lasers, with energy resolution of about 10^{-5} eV, may be used directly, or they may be used to pump a tunable dye laser with energy resolution of about 10^{-3} eV in the present configuration. R6G, R640, and R110 dyes were used with argon ion laser pumping. Oxazine perchlorate was used with krypton ion laser pumping. The violet and ultraviolet lines of the krypton ion laser were selected by mirror coating only, rather than with a prism as was done with the other laser lines. Since this method is not as definitive as a wavelength selector, the lines at 415.4 and 413.1 nm lased simultaneously with the violet mirrors as did the lines at 356.4 and 350.7 nm with the ultraviolet mirrors.

A microcomputer has been interfaced to the experiment to facilitate data gathering when operating with the tunable dye laser. Here measurements are made at 1 nm intervals. The microcomputer moves the dye laser these 1 nm increments, sets the mass spectrometer to the appropriate mass, and gathers data on the counters until a preselected statistical error criterion is met. Upon completion of the data taking for each photon wavelength the microcomputer calculates the photodestruction cross section together with the statistical uncertainty of the measurement. Further details concerning the microcomputer control of this experiment will be published elsewhere.[8]

---

[7] R. A. Beyer and J. A. Vanderhoff, "Cross Section Measurements for Photodetachment or Photodissociation of Ions Produced in Gaseous Mixtures of O_2, CO_2, and H_2O," J. Chem. Phys. 65, 2313-2321 (1976).

[8] L. M. Colonna-Romano, "Microcomputer Automation of the BRL Photodestruction Experiment," BRL Report in preparation.

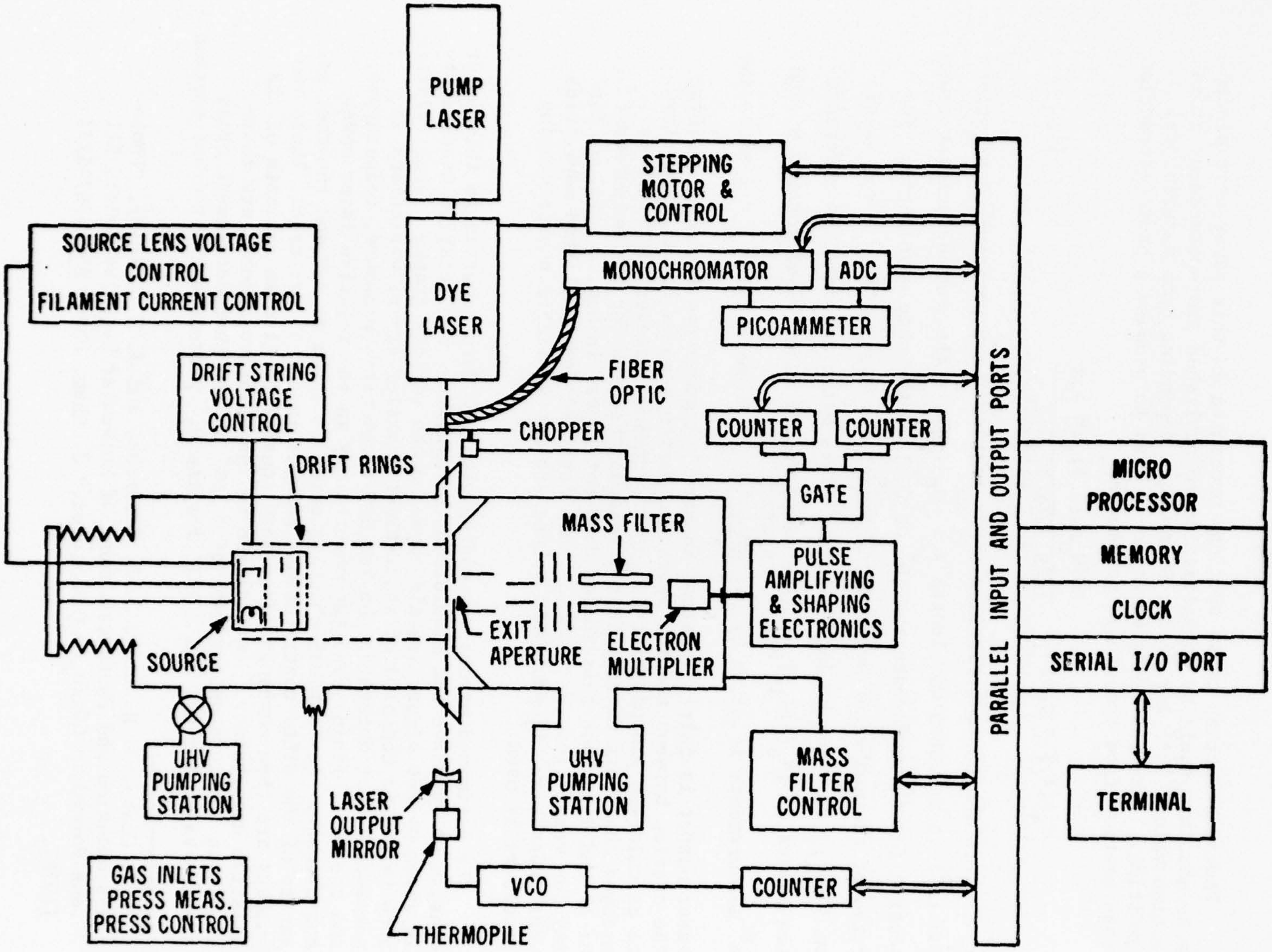

Figure 1. Schematic diagram of the experimental apparatus.

ANALYSIS

Photodestruction cross sections presented in this paper were placed on an absolute scale by normalization to published photodetachment cross section values[6,7,9] for either O^- or O_2^- depending upon experimental conditions. The following equation is used to produce a photodestruction cross section from measurable parameters:

$$\sigma_{A^\pm}(\lambda_1) = \sigma_{R^-}(\lambda_1) \; \frac{\ln[N_o/N(\lambda_1)]_{A^\pm} \underline{P} \; v_{A^\pm}}{\ln[N_o/N(\lambda_1)]_{R^-} \; v_{R^-}} \quad . \qquad (1)$$

$\sigma_{A^\pm}(\lambda_1)$ is the photodestruction cross section for a positive or negative ion ($A^\pm$) at a photon wavelength λ_1. $\sigma_{R^-}(\lambda_1)$ is the photodetachment cross section for the reference ion (O^- or O_2^-) at the same wavelength. The ratio of the number of detected $A^\pm$ counts for laser off (N_o) and laser on ($N(\lambda_1)$) is given by $[N_o/N(\lambda_1)]_{A^\pm}$. This ratio for detected reference ion counts is $[N_o/N(\lambda_1)]_{R^-}$. The ratio of the laser power for the R^- and $A^\pm$ measurements is given by $\underline{P} = \dfrac{P_{R^-}(\lambda_1)}{P_{A^\pm}(\lambda_1)}$. In most cases $\underline{P} = 1$ since the laser output is fairly constant in time. A geometric factor describing the overlap between the ion swarm and photon beam is normally required to calculate a photodestruction cross section; however, it has been assumed that this overlap factor remains the same for the measurement of $A^\pm$ and R^-. Thus this factor does not appear in Eqn. 1. Values for the ion velocities, $v_{A^\pm}$ and v_{R^-}, are obtained from published mobilities where possible. If published values are not available a mass scaling procedure is used.[7]

The estimated errors associated with the data reported in this paper consist of relative and absolute uncertainties. The relative uncertainty is given by the error bars displayed on the various graphs. This relative uncertainty is composed of statistical counting error, variations in parameters that determine the ion drift velocity (pressure, temperature, and the drift field), and the uncertainty in the relative laser power measurement. Statistical counting error is taken as $\pm\sqrt{N}$ and the root mean square of the other contributions results in a ± 5% estimate. These two numbers are then combined (root mean square) to give an estimate of the relative uncertainty. In addition to the relative uncertainty there exists an absolute uncertainty of ± 10%[4] in the photodetachment cross section value for O^-, and ± 13%[7] for the O_2^- photodetachment cross section.

---

[9] P. C. Cosby, J. H. Ling, J. R. Peterson, and J. T. Moseley, "Photodissociation and Photodetachment of Molecular Negative Ions: III. Ions Formed in $CO_2/O_2/H_2O$ Mixtures," J. Chem. Phys. 65, 5267-5274 (1976).

An absolute uncertainty also exists in the reduced mobilities used to compute the ion drift velocities. These reduced mobilities, the associated error, and the method of determination are given in Table 1. A conservative absolute uncertainty of ± 20% was assigned to reduced mobilities obtained by mass scaling. Combining the absolute uncertainty in the photodetachment cross section of the reference ion with the uncertainty in the reduced mobility in a root mean square sense gives the absolute uncertainty. The total error must be computed point by point.

RESULTS

This section is divided into four parts depending on the type of photodestruction mechanism available to the ions studied: negative ions that can photodetach only, negative ions that can photodetach and/or photodissociate, positive ions that may charge transfer, and other positive ions.

Due to energetic considerations the negative molecular ions O_2^-, NO_2^-, and SO_2^- can undergo only photodetachment for the range of photon energies used in this experiment. A number of photodetachment experiments have been performed on O_2^- many of which have used broad band radiation or collimated negative ion beams.[6,11,12] Cosby et al.[9] and Beyer and Vanderhoff[7] have measured photodetachment cross sections for thermal (300°K) O_2^- ions using high resolution laser photon radiation. The results of these measurements are displayed on Fig. 2. See Ref. 7 for details of O_2^- preparation. A dye laser was used for the 750 to 700 nm and 625 to 575 nm regions and the error bar approximately centered within each respective cluster of dots represents the total relative error for these measurements. Violet lines (415.4/413.1 nm) of a krypton ion laser were used for the high photon energy point. The O_2^- measurements were normalized to the photodetachment cross section for O^- hence the root mean square absolute error is ± 11% and the root mean square total error is estimated as ±16%. At several photon wavelengths the drift distance, E/N, gas pressure, and laser power were varied with no noticeable effects on the photodetachment cross section for O_2^-. This suggests that the ions are thermalized and possible chemistry and diffusion effects are negligible. These results are in good agreement with Cosby et al. and with published beam data.[6,12] Over the photon wavelength range 750 to 413 nm the photodetachment cross section appears unstructured.

---

[10] E. W. McDaniel and E. A. Mason, The Mobility and Diffusion of Ions in Gases, p. 291 (Wiley, New York, 1973).

[11] S. B. Woo, L. M. Branscomb, and E. C. Beaty, "Sunlight Photodetachment Rate of Ground State O_2^-," J. Geophys. Res. 96, 2933-2940 (1969) and references contained therein.

[12] D. S. Burch, S. J. Smith, and L. M. Branscomb, "Photodetachment of O_2^-," Phys. Rev. 112, 171-175 (1958).

TABLE 1. ZERO-FIELD REDUCED MOBILITIES (K_0) FOR VARIOUS IONS AT 300°K IN O_2 GAS*

Ion	$K_o(\frac{cm^2}{V\text{-}s})$	Method
O^-	3.20±0.09	Drift tube mass spectrometer
O_2^-	2.16±0.07	Drift tube mass spectrometer
O_3^-	2.55±0.08	Drift tube mass spectrometer
O_4^-	2.14±0.08	Drift tube mass spectrometer
CO_3^-	2.50±0.07	Drift tube mass spectrometer
CO_4^-	2.45±0.07	Drift tube mass spectrometer
SO_2^-	2.48	Mass Scaled
SO_4^-	2.33	Mass Scaled
$O_2^-(H_2O)$	2.55	Mass Scaled
$O_2^+(O_2)$	2.16±0.08	Drift tube mass spectrometer
$O_2^+(SO_2)$	2.33	Mass scaled
$O_2^+(CO_2)$	2.45	Mass scaled
$H^+(H_2O)$	3.20	Mass Scaled
$H^+(H_2O)_2$	2.68	Mass Scaled
$H^+(H_2O)_3$	2.50	Mass Scaled
$H^+(H_2O)_4$	2.45	Mass Scaled

*Experimentally measured mobility values were taken from a table in McDaniel and Mason.[10]

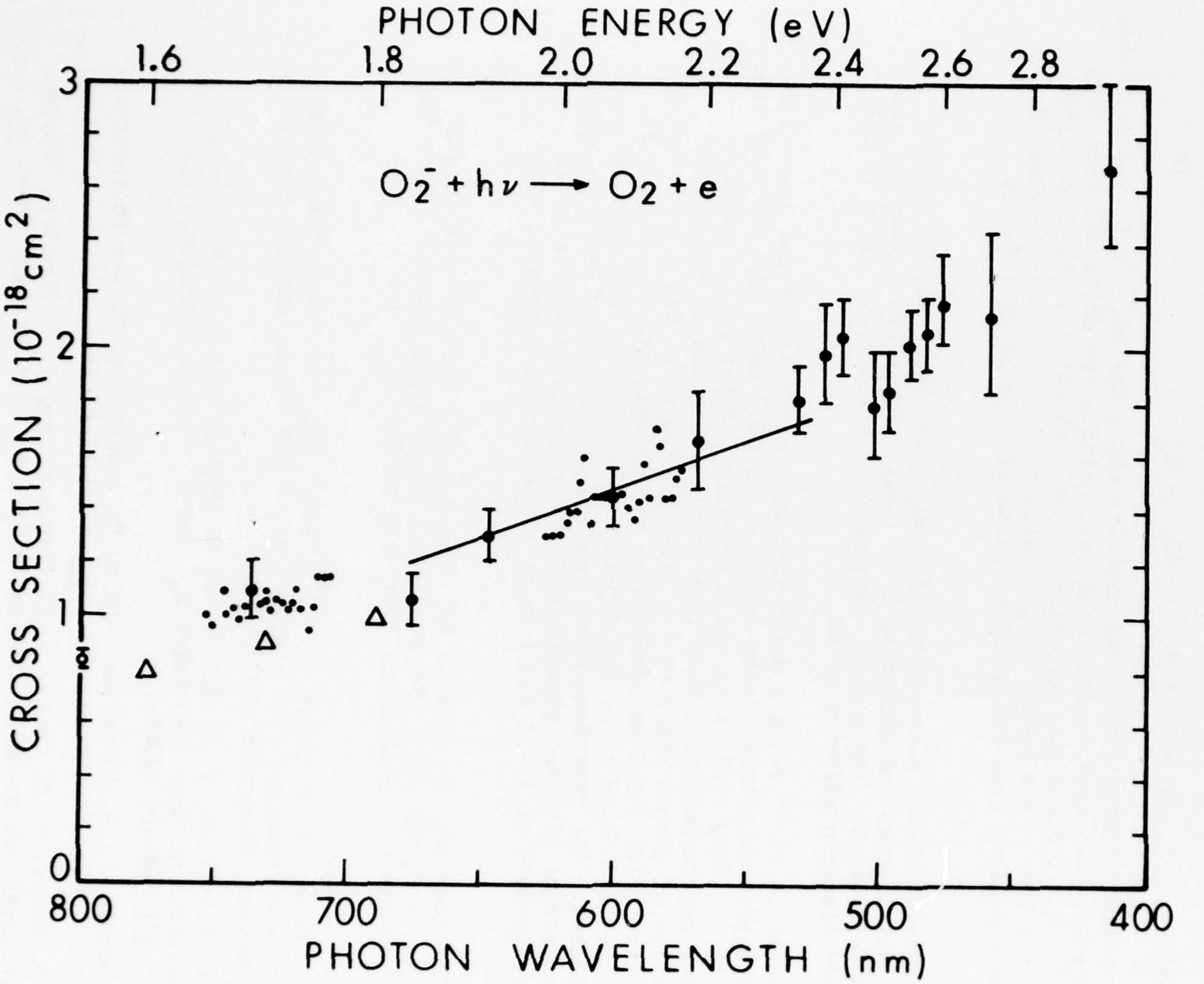

Figure 2. Photodetachment cross section for O_2^- as a function of photon wavelength. The E/N ranged from 10 to 15 x 10^{-17} V-cm^2. The solid line and triangles approximate the tunable dye laser data of Cosby et al.[9,13] and the dots with associated error bars covering the 676.4 to 457.9 nm region represents the discrete ion laser data of Beyer and Vanderhoff.[7] The dots in the region 750 to 700 nm, 625 to 575 nm, as well as the point at 415.4/413.1 nm represent present results.

The NO_2^- ion has been briefly investigated. By using gas mixtures of oxygen and nitric oxide (13.3 N/m^2), where O_2 comprised 98% or more of the mixture, NO_2^- was produced through the reactions

$$O_2 + e \rightarrow O^- + O \qquad \text{I}$$

and

$$O^- + NO + O_2 \rightarrow NO_2^- + O_2 \qquad \text{II}$$

Since no experimentally measured mobility value for NO_2^- in O_2 was available measurements were made to determine this using a two drift distance technique.[14] K_0 at 300°K was determined to be 2.85 cm^2/V-s with a probable error of ± 10%. As a comparison, a value of 2.63 cm^2/V-s is obtained when mass scaling from the mobility value of 2.50 cm^2/V-s for CO_3^- in O_2.

Photodetachment measurements for NO_2^- have been made at several photon wavelengths and differing E/N values. These cross sections are listed in Table 2. The photon wavelength of 514.5 nm is close to the reported electron affinity of NO_2^-.[15]

Huber et al.[16] using a drift tube mass spectrometer and laser have observed photodetachment cross sections for NO_2^- below the reported electron affinity.[15] They find these cross sections exhibit an E/N and drift distance dependence which they interpret as evidence of vibrational excitation of ground state NO_2^-. Present results at 514.5 nm (slightly above threshold) could be affected by vibrational excitation as well since they are found to be E/N dependent. Drift distance dependence was not checked. The photodetachment results at 488.0, and 457.9 nm are in good agreement with the experimental measurements of Herbst et al.[15] and the measurement at 415.4/413.1 nm is in reasonable agreement with Warneck.[6]

The ions SO_2^- as well as SO_4^- and $O_2^+(SO_2)$ were created in gas mixtures of O_2 and SO_2. The proportions were approximately 1 part SO_2 to 7600 parts O_2. Mechanisms available to form SO_2^- are

---

[13] P. C. Cosby, G. P. Smith, J. T. Moseley, and L. C. Lee, "Photodissociation of Atmospheric Positive Ions," 30th Annual Gaseous Electronics Conference, MA-6, Oct. 1977.

[14] D. L. Albritton, T. M. Miller, D. W. Martin, and E. W. McDaniel, Mobilities of Mass Identified H_3^+ and H^+ Ions in Hydrogen," Phys. Rev. 171, 94-102 (1968).

[15] E. Herbst, T. A. Patterson, and W. C. Lineberger, "Laser Photodetachment of NO_2^-," J. Chem. Phys. 61, 1300-1304 (1974).

[16] B. A. Huber, P. C. Cosby, J. R. Peterson, and J. T. Moseley, "Photodetachment and De-excitation of Excited NO_2^{-*}," J. Chem. Phys. 66, 4520-4526 (1977).

TABLE 2. PHOTODETACHMENT CROSS SECTIONS FOR NO_2^-.

Photon Wavelength (nm)	E/N ($V\text{-}cm^2$)	σ ($10^{-18} cm^2$)	Relative Error ($10^{-18} cm^2$)
514.5	11.5	0.27	0.06
488.0	11.5	0.28	0.06
457.9	11.5	0.49	0.14
457.9	23	0.50	0.21
514.5	23	0.25	0.06
514.5	34.5	0.37	0.08
514.5	46	0.45	0.08
*356.4/350.7	15	4.90	0.88

*The photodetachment cross section measured at 356.4/350.7 nm was normalized to the photodetachment cross section for O_2^- (Warneck[6] measured this value as 3.6×10^{-18} cm^2). The other wavelengths were normalized with the photodetachment cross section for O^-.

$e + O_2 \rightarrow O^- + O$ I

and $e + 2O_2 \rightarrow O_2^- + O_2$ III

followed by $O^- + O_2 \rightarrow O_2^- + O$ IV

$O^- + SO_2 \rightarrow SO_2^- + O$ V

and $O_2^- + SO_2 \rightarrow SO_2^- + O_2$. VI

Results of the photodestruction cross section measurements are displayed on Fig. 3. The photodestruction cross section is due entirely to photodetachment since the photon energy region is indufficient to produce photodissociation by a one photon interaction. The experimental parameters were a gas pressure of 40 N/m^2, $E/N = 10^{-16}$ $V\text{-}cm^2$, and a drift distance of 5.6 cm. These measurements were normalized to O^- however several checks were made by normalization to O_2^- and these checks gave the same results as for the O^- normalization. Concentrations of O_3^- present were insufficient to give normalization difficulties through a production channel for O^-, namely photodissociation of O_3^- to O^- and O_2. As will be shown later the photodestruction cross section for SO_4^- is small or zero hence cannot alter the SO_2^- results. Drift distance, E/N, and gas pressure were varied at a fixed photon wavelength and no noticable changes were observed in the SO_2^- photodetachment cross section.

The photon energy region of experimental investigation is well above the reported threshold for photodetachment (1.1 eV).[17,18] The photodetachment cross section for SO_2^- exhibits a slow increase with decreasing wavelength and no evidence of structure is apparent from the results of Fig. 3. As a comparison Feldman[18] has measured the photodetachment cross section for SO_2^- over this wavelength region using a broadband light source and a beam apparatus. He observes cross section values which are about a factor of two larger than those presented here and are essentially constant over the photon energy range from 1.6 to 2.5 eV. At about 2.6 eV Feldman observes a sharp increase in the SO_2^- cross section which does not appear in the drift tube data. Several tests were performed to determine if the SO_2^- produced in the drift tube was excited. Variation of drift distance, pressure, or E/N at a fixed photon wavelength did not have any influence on the measured cross sections suggesting that the SO_2^- formed in the drift tube was thermalized. A likely effect giving rise to the magnitude difference is vibrational excitation of SO_2^- produced in beam conditions. As Feldman points out, the flatness in the photodetachment cross section for SO_2^- can result from vibrational excitation.

---

[17] R. J. Celotta, R. A. Bennett, and J. L. Hall, "Laser Photodetachment Determination of the Electron Affinities of OH, NH_2, NH, SO_2, and S_2," J. Chem. Phys. 60, 1470-1745 (1974).

[18] D. Feldman, "Photoablösung von Elektronen bei einigen Stabilen Negativen Ionen," Z. Naturforsch 25a, 621-626 (1970).

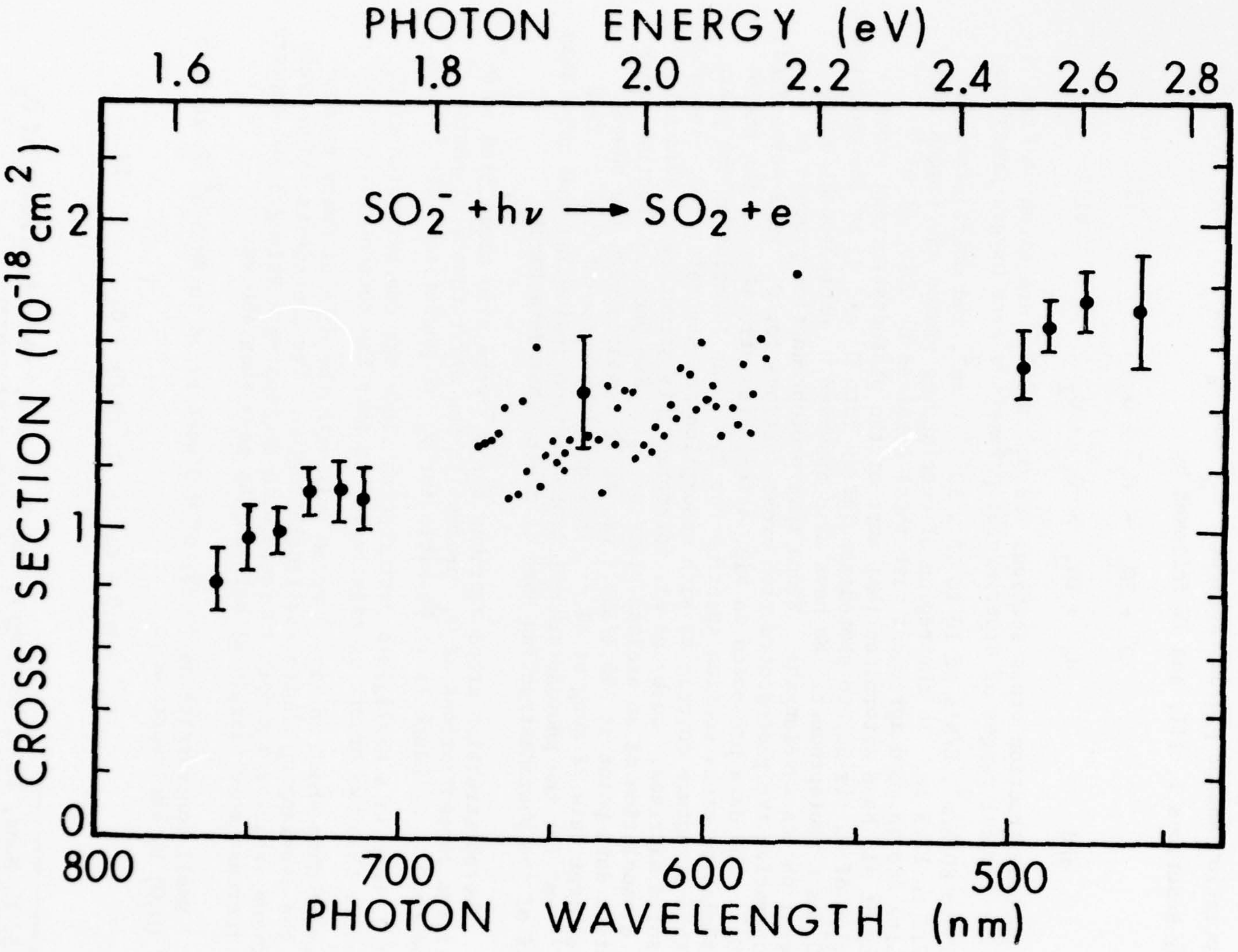

Figure 3. Photodetachment cross section for SO_2^- as a function of photon wavelength. The points from 760 to 570 nm are dye laser points. The other points are from the discrete lines of an argon ion laser, all present results.

The ions O_3^-, O_4^-, $O_2^-(H_2O)$, SO_4^-, and CO_4^- can undergo both photodissociation and/or photodetachment. O_3^- and O_4^- were created in pure O_2 by Reactions I, III, and IV followed by

$$O^- + 2O_2 \rightarrow O_3^- + O_2 \qquad \text{VII}$$

and

$$O_2^- + 2O_2 \rightarrow O_4^- + O_2 \qquad \text{VIII}$$

The photodestruction cross sections for O_3^- and O_4^- are given on Figs. 4 and 5. Typical ranges of experimental parameters were oxygen pressures of 53 to 80 N/m^2, E/N's of 10 to 15 x 10^{-17} V cm^2, and drift distances of 7.5 to 11.3 cm. In the region of overlapping photon wavelength these results are in good agreement with those obtained by Cosby et al.[9] Cosby et al. have determined that most of the photodestruction cross section of O_3^- is due to photodissociation into O^- and O_2 by the observance of O^- as a photoproduct. We have also observed O^- photoproduction at several photon wavelengths. Since this photoproduction process of O^- is operative the photodestruction cross sections for O_3^- were normalized to O_2^-. The data presented on Fig. 4 indicates structure in the photodissociation cross section spectrum for O_3^-. The location of the peaks in this structure correlates with absorption measurements of O_3^- isolated in solid matrices. Cosby et al. interpret this structure as evidence for dissociation of an excited state of O_3^-. The photodestruction cross section data point at 356.4/350.7 nm can be compared with the photodetachment data of Wong et al.[19] They obtain a value of 1.15 ± .25 x 10^{-18} cm^2 for the photodetachment cross section indicating that more than half of the photodestruction here is due to photodetachment.

Photodestruction cross sections for O_4^- were also normalized to O_2^- as large concentrations of O_3^- present in the drift tube will photoproduce O^-. Although it is possible for O_4^- to photodissociate into O_2^- and O_2 this is a negligible perturbation since the concentration of O_4^- is more than two orders of magnitude less than the concentration of O_2^-. Present data shown in Fig. 5 agree well with the data of Cosby et al.[9] in the overlapping photon wavelength region. The photodestruction cross section exhibits a smooth increase with decreasing wavelength and appears to increase more sharply at wavelengths less than 450 nm.

Small concentrations (~ 2%) of H_2O were added to 80 N/m^2 O_2 to form $O_2^-(H_2O)$ by the reaction

$$O_2^- + H_2O + O_2 \rightarrow O_2^-(H_2O) + O_2. \qquad \text{IX}$$

---

[19] S. F. Wong, T. V. Vorburger, and S. B. Woo," Photodetachment of O_3^- in a Drift Tube," Phys. Rev. A 5, 2598-2604 (1972).

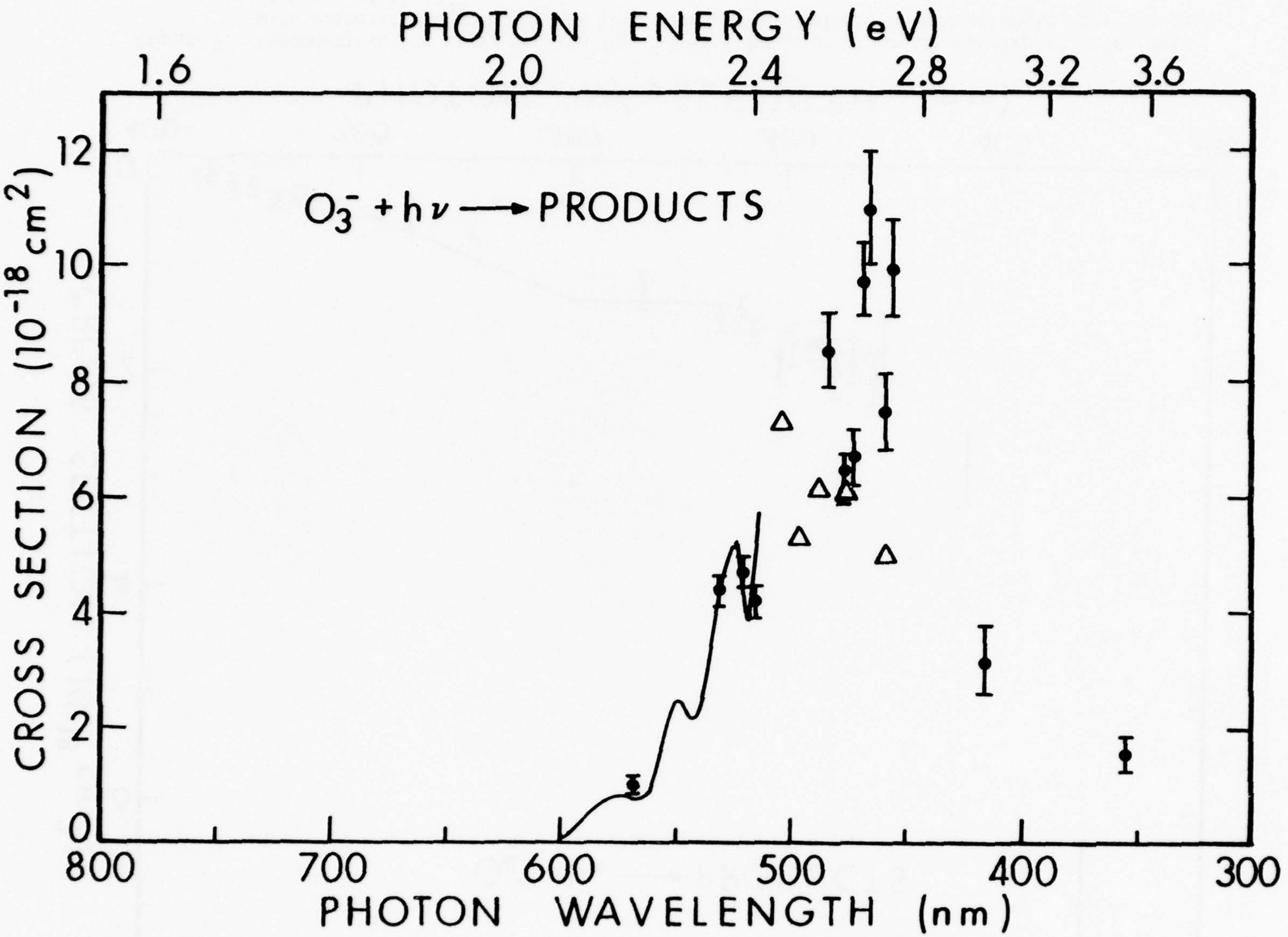

Figure 4. Photodestruction cross section for O_3^- as a function of photon wavelength. The dots with associated error bars are this work and the solid line and triangles approximate the data of Cosby et al.[9]

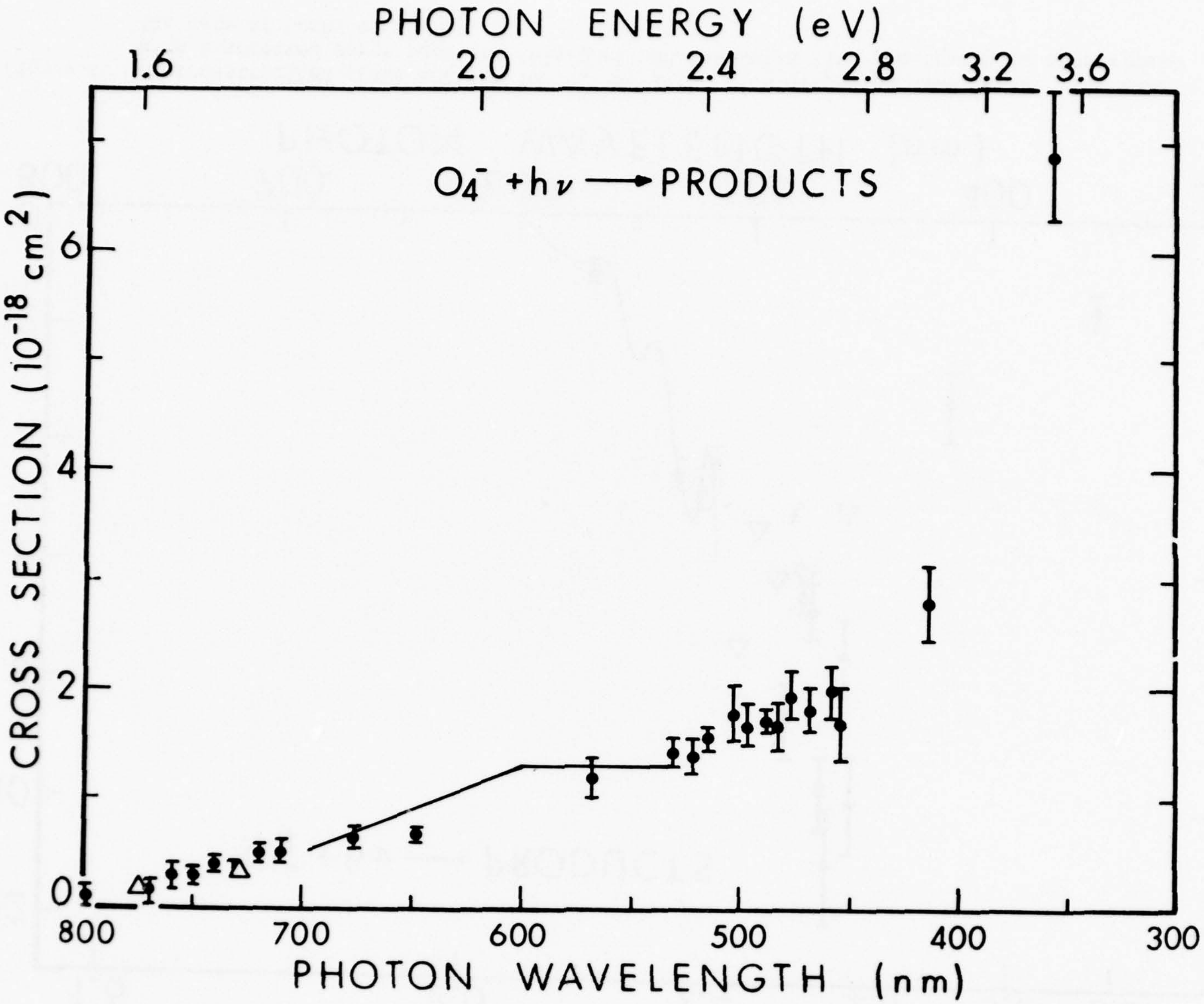

Figure 5. Photodestruction cross section for O_4^- as a function of photon wavelength. The dots with associated error bars are this work and the solid line and triangles are the data of Cosby et al.[9,13]

The photodestruction cross section of $O_2^-(H_2O)$ is displayed on Fig. 6. A drift distance of 7.5 cm and an E/N of 11.5×10^{-17} V cm^2 were used for these measurements. O_2^- was used for normalization and here also possible effects of $O_2^-(H_2O)$ photodissociating into O_2^- and H_2O are negligible due to the small concentration of $O_2^-(H_2O)$ present. Again data of Cosby et al.[9] is shown for comparison.

Gas mixtures of O_2 and SO_2 (the same composition and pressure as in the SO_2^- measurements) were used for forming SO_4^- by the reaction

$$O_2^- + SO_2 + O_2 \rightarrow SO_4^- + O_2 . \qquad X$$

No photodestruction of SO_4^- was observed for any of the photon wavelengths studied and upper limits on the photodestruction process was established from the relative error in the measurement. These upper limits are listed in Table 3.

CO_4^- was formed from gas mixtures of O_2 and CO_2 by the reaction

$$O_2^- + CO_2 + M \rightarrow CO_4^- + M \qquad XI$$

where M is O_2 or CO_2.

The gas composition was approximately half CO_2. No photodestruction cross sections were observed hence upper limits were established and are listed in Table 4. These measurements were normalized to O_2^- since the large quantities of CO_3^- present[20] can photodissociate to produce an O^- photoproduct. Cosby et al.[9] have investigated CO_4^- from 690 to 514.5 nm and have established upper limits for the photodestruction cross section. At 520 and 514.5 nm they observe a photodestruction cross section of .025 and .037 x $10^{-18} cm^2$, respectively. Vestal[21] has measured the photodissociation of CO_4^- from 600 to 305 nm and finds the cross section increasing from 0.07×10^{-18} cm^2 at 530 nm to 0.28×10^{-18} cm^2 at 305 nm.

Many weakly bound positive ion clusters (binding energy < 1.0 eV) have been found to photodissociate readily. These ions include $O_2^+(CO_2)$,[7,22]

---

[20] J. T. Moseley, P. C. Cosby, and J. R. Peterson, "Photodissociation Spectroscopy of CO_3^-," J. Chem. Phys. 65, 2512-2517 (1976), and references contained therein.

[21] M. L. Vestal, "Fundamental Research Relating to New Laser Systems," Final Report on Air Force Contract F33615-73-C-4128, March 1976.

[22] G. P. Smith, P. C. Cosby, and J. T. Moseley, "Photodissociation of Atmospheric Positive Ions I. 5300-6700Å," J. Chem. Phys. 67, 3818-3828 (1977).

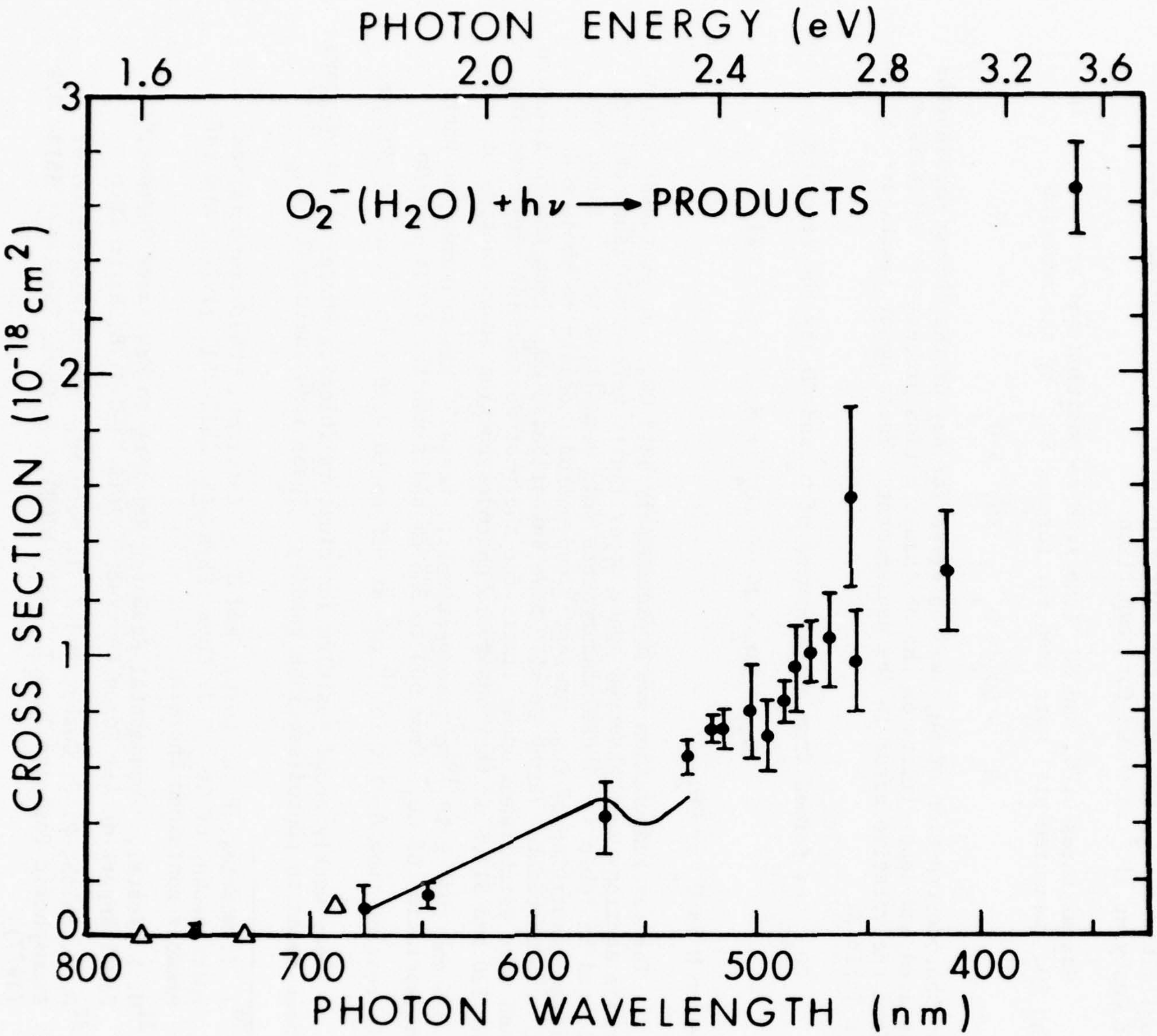

Figure 6. Photodestruction cross section for $O_2^-(H_2O)$ as a function of photon wavelength. Dots with associated error bars are this work.[2] The solid line and triangles are the data of Cosby et al.[9,13]

TABLE 3. PHOTODESTRUCTION CROSS SECTION UPPER LIMITS FOR SO_4^-.
E/N = 10^{-16} V-cm^2

Wavelength (nm)	Cross Section Upper Limit (10^{-18} cm^2)
760	0.11
750	.05
740	.08
730	.08
720	.10
670	.20
660	.10
650	.11
640	.09
630	.06
620	.16
610	.07
600	.04
590	.04
580	.05
570	.26
496.5	.07
488.0	.10
476.5	.08
457.9	.09
687.5	.09

TABLE 4. PHOTODESTRUCTION CROSS SECTION UPPER LIMITS FOR CO_4^- IN UNITS OF 10^{-18} cm^2, $E/N = 15 \times 10^{-17}$ $V\text{-}cm^2$.

Wavelength (nm)	Cross Section Upper Limits
799.3	.07
752.5	.03
720.0	.06
695.0	.15
415.4/413.1	.08

$O_2^+(H_2O)_{1,2}$[7,22,23] $O_2^+(SO_2)$, $O_2^+(O_2)$,[7,21-23] $NO^+(NO)$[22-24] and $CO_2^+(CO_2)$.[21,22] The range of photon energies used in this experiment is sufficient to cause $O_2^+(CO_2)$, $O_2^+(H_2O)_{1,2}$, and $O_2^+(SO_2)$ to charge transfer upon photodissociation. Thus in addition to the exothermic photodissociation channel

$$O_2^+(M) + h\nu \rightarrow O_2^+ + M \qquad \text{XII}$$

there exists the exothermic channel

$$O_2^+(M) + h\nu \rightarrow O_2 + M^+ \, . \qquad \text{XIII}$$

The $O_2^+(CO_2)$ ion directly exhibits this property. From previous studies[7,22] a photoproduct CO_2^+ has been observed when irradiating $O_2^+(CO_2)$ clusters with photons of energy exceeding 2.0 eV. Photodissociation cross section measurements for the $O_2^+(CO_2)$ clusters have been extended in wavelength and these results are listed in Table 5. The experimental parameters are similar to those described in Ref. 7.

Direct evidence of a charge transfer reaction for $O_2^+(H_2O)_{1,2}$ or $O_2^+(SO_2)$ was not observed. However this does not preclude its existence since in contrast to the $O_2^+(CO_2)$ measurements where CO_2 was the dominant gas, here O_2 was the dominant gas and thus fast charge transfer reactions

$$SO_2^+ + O_2 \rightarrow O_2^+ + SO_2 \qquad \text{XIV}$$

and

$$H_2O^+ + O_2 \rightarrow O_2^+ + H_2O \qquad \text{XV}$$

can occur prior to detection. Photodissociation cross sections for $O_2^+(H_2O)$ at extended photon wavelengths are given in Table 6. The photodissociation cross section values for $O_2^+(H_2O)$ at 676.4 and 647.1 nm are smaller than those reported previously. The mechanism believed responsible for the high values reported previously is an equilibrium effect with another photodissociating ion $O_2^+(O_2)$. Details of this effect is described elsewhere.[23,24] Photodissociation of $O_2^+(SO_2)$ has not been reported previously. This ion cluster was produced using the same gas mixture as used for the case of SO_2^- described earlier.

---

[23] R. R. Burke and R. P. Wayne, "Photodissociation of Positive Cluster Ions by CW and Pulsed Laser Radiation," Int. J. Mass. Spectr. Ion Phys. 25, 199-209 (1977).

[24] J. A. Vanderhoff, "Photodissociation of $NO^+(NO)$ and $NO^+(H_2O)$," J. Chem. Phys. 67, 2332-2337 (1977).

TABLE 5. PHOTODISSOCIATION CROSS SECTIONS FOR $O_2^+(CO_2)$.
E/N = 15 x 10^{-17}V-cm^2.

Wavelength (nm)	Cross Section (10^{-18} cm^2)	Relative Error (10^{-18} cm^2)
799.3	0.00	0.06
752.5	-0.02	0.05
413.1/415.4	3.00	0.25
356.4/350.7	2.19	0.14

TABLE 6. PHOTODISSOCIATION CROSS SECTIONS FOR $O_2^+(H_2O)$.
E/N = 15 x 10^{-17} V-cm^2.

799.3	0.00	0.06
752.5	-0.01	0.05
676.4	0.03	0.05
647.1	0.10	0.08
413.1/415.4	5.60	0.35
356.4/350.7	11.06	0.63

The reactions

$$O_2^+ + SO_2 + O_2 \rightarrow O_2^+(SO_2) + O_2 \qquad \text{XVI}$$

and

$$O_2^+ + 2O_2 \rightarrow O_2^+(O_2) + O_2 \qquad \text{XVII}$$

followed by

$$O_2^+(O_2) + SO_2 \rightarrow O_2^+(SO_2) + O_2 \qquad \text{XVIII}$$

are responsible for forming this ion.

The photodissociation data for $O_2^+(SO_2)$ are displayed on Fig. 7, where the E/N was held fixed at 30 x 10^{-17} V cm^2 and the drift distance fixed at 5.6 cm. The photodissociation cross section at a fixed photon wavelength was found to be independent of E/N, laser power, pressure, and drift distance suggesting the cluster ion is thermalized and effects of chemistry and diffusion are negligible. This cross section appears to vary smoothly with photon wavelength and has a maximum between 520 and 580 nm decreasing in value on either side.

The "dimer" ions $NO^+(NO)$, $O_2^+(O_2)$, and $CO_2^+(CO_2)$ exhibit large photodissociation cross sections that vary smoothly with photon wavelength. Results for the photodissociation cross section of $NO^+(NO)$ have been reported previously.[24] Extended measurements together with published measurements for $O_2^+(O_2)$ are shown in Fig. 8. Experimental conditions were arranged analogous to those reported in Ref. 7. No variation in cross section occurred when E/N, pressure, or drift distance for a fixed photon wavelength, however there was a dependence on laser power. In wavelength regions where the cross section is large coincident with high laser powers the cross section became slightly dependent on laser power. For these cases the cross section was measured at several laser powers and the reported cross section was obtained by a linear extrapolation to zero laser power. There is no detailed structure for the $O_2^+(O_2)$ photodissociation cross section exhibited on Fig. 8 indicating the photodissociation process is due to excitation of $O_2^+(O_2)$ to a purely repulsive state of the cluster. However, two broad maxima in the photodissociation cross section are suggested, one at ~ 1.5 eV the other at photon energies slightly greater than 3.6 eV. This could be explained by two repulsive states of the $O_2^+(O_2)$ cluster which are separated by this photon energy difference.

We have observed a large photodissociation cross section (~ 10^{-17} cm^2) for $CO_2^+(CO_2)$ at a photon wavelength of 600 nm. A more complete investigation has been accomplished by Vestal[21] who observes the photodissociation cross of $CO_2^+(CO_2)$ to vary from 25 to 1.8 x 10^{-18} cm^2 over the wavelength region from 627 to 305 nm and Cosby et al.[13] who find the photodissociation cross section to vary from 10.2 to 23.0 x 10^{-18} cm^2 over the wavelength region from 820 to 590 nm.

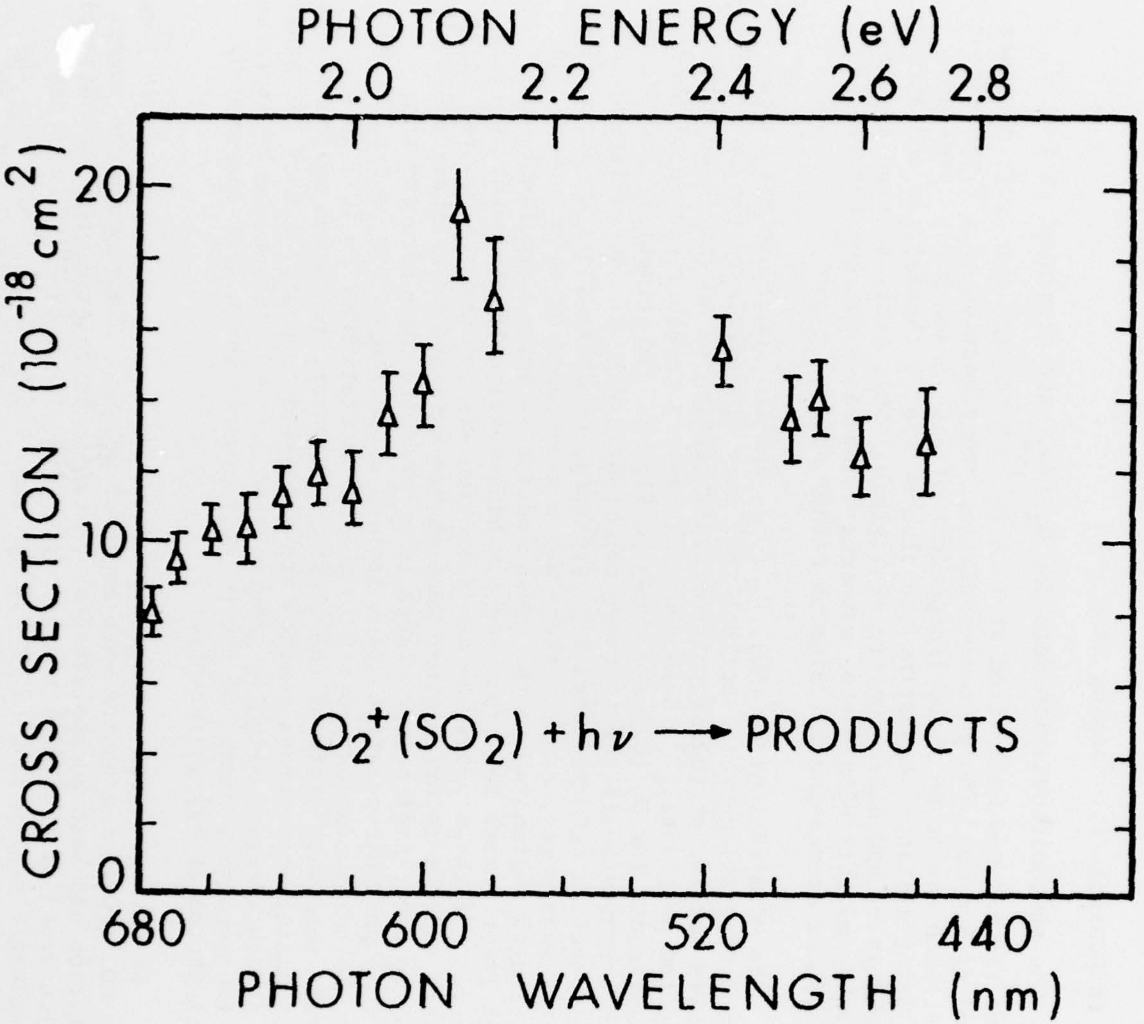

Figure 7. Photodissociation cross section for $O_2^+(SO_2)$ as a function of photon wavelength, this work.

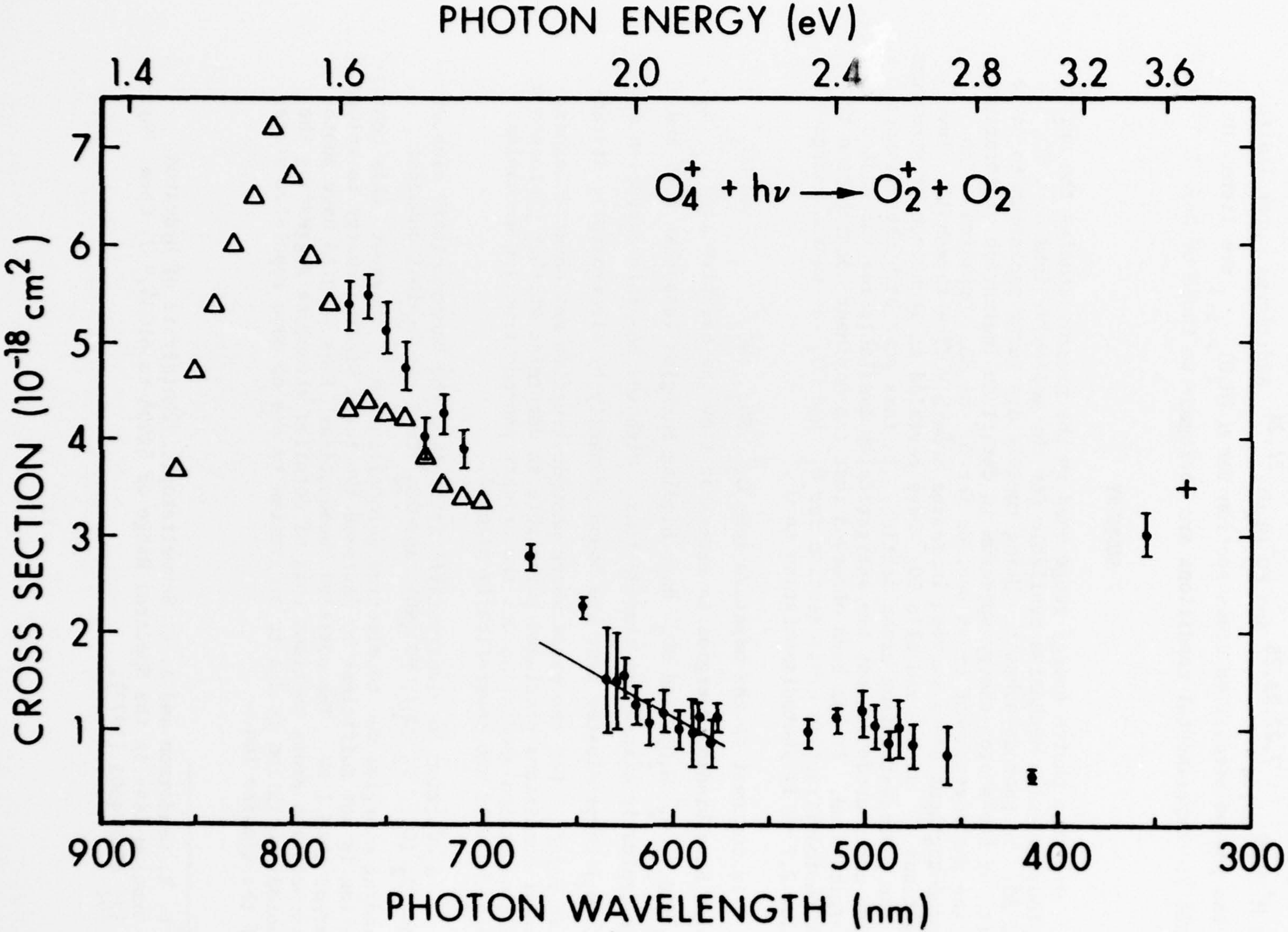

Figure 8. Photodissociation cross section for $O_2^+(O_2)$ as a function of photon wavelength. The points with associated error bars are this work. The solid line and triangles are the data of Cosby et al.[9,13] The point at 337.1 nm is data of Burke and Wayne.[23]

Positive ion clusters for which no photodissociation has been observed are $H^+(H_2O)_{n=1-4}$[7,22,23,25] and $NO^+(H_2O)$.[22,24] Additional upper limits on the photodissociation cross section for $H^+(H_2O)_{n-1-4}$ are listed in Table 7. Experimental conditions are analogous to those of Ref. 7.

SUMMARY

Over the photon energy range used in the present studies the only photodestruction mechanism available for the molecular ions O_2^-, NO_2^- and SO_2^- is photodetachment. Using tunable dye laser radiation to cover parts of the photon energy spectrum in detail no indication of structure in the photodetachment cross section for O_2^- or SO_2^- appeared. The photodetachment cross section increases smoothly from threshold. Investigations[9,20] of O_3^- and also CO_3^- have revealed an abundance of structure in the photodestruction cross section. In this case both photodissociation and photodetachment are energetically available for the photon energies used. It has been observed that the dominant contribution to the photodestruction cross section for O_3^- and CO_3^- at photon energies below 2.7 eV is photodissociation to O^-.

In contrast to the negative ions O_2^-, SO_2^-, NO_2^-, O_3^-, and CO_3^- which have binding energies in excess of 1 eV the negative ions $O_2^-(O_2)$, $O_2^-(CO_2)$, $O_2^-(H_2O)$, and SO_4^- have binding energies less than 1 eV and are typically classed as cluster ions. With the possible exception of $O_2^-(O_2)$ these cluster ions are bound primarily by electrostatic attractive forces. For the cases where photodestruction was observed experimental conditions precluded being able to determine whether photodetachment or photodissociation was the primary photodestruction mechanism. Both channels are energetically allowed.

In addition to electrostatic attraction the "homonuclear" cluster ions $O_2^-(O_2)$, $O_2^+(O_2)$, $NO^+(NO)$, and $CO_2^+(CO_2)$ can exhibit enhanced binding energies due to electron delocalization.[26] However, this contribution is not sufficient to increase the total binding energy to values larger than 1 eV. The positive "homonuclear" ions studied have photodissociation cross sections void of detailed structure suggesting the photodissociation is due to excitation to one or more repulsive states of the cluster ion.

---

[25] W. R. Henderson and A. L. Schmeltekopf, "Photolysis of Hydrated Oxonium Ions in the Spectral Range of 5800Å to 6100Å," J. Chem. Phys. 57, 4502-4503 (1972).

TABLE 7. PHOTODISSOCIATION CROSS SECTION UPPER LIMITS FOR $H^+(H_2O)_{n=1-4}$.

Wavelength (nm)	$H^+(H_2O)$ $(10^{-18} cm^2)$	$H^+(H_2O)_2$ $(10^{-18} cm^2)$	$H^+(H_2O)_3$ $(10^{-18} cm^2)$	$H^+(H_2O)_4$ $(10^{-18} cm^2)$
799.3	.09	.06	.06	.06
752.5	-	.04	.13	.10
413.1/415.4	.04	.10	.04	.06
356.4/350.7	.08	.09	.06	.07

Photodissociation was not observed for either $NO^+(H_2O)$ or $H^+(H_2O)_{n=1-4}$. Here the photon energy range covered did not reach values sufficient for charge transfer to occur. Photodissociation studies[13] have been made on $NO^+(N_2)$, $NO^+(CO_2)$, and $NO^+(NO_2)$ where the photon energy used was not sufficient to allow a charge transfer (Reaction XIII) to be energetically allowed. No photodissociation was observed for these cases. Thus it may be that weakly bound positive cluster ions photodissociate predominantly by a charge transfer channel.

REFERENCES

1. L. Thomas, P. M. Gondhalecar and M. R. Bowman, "Photodetachment of Electrons from Negative Ions in the Lower D Region," Nature 238, 89-90 (1972).

2. L. Thomas and M. R. Bowman, "A Theoretical Study of Negative Ion Changes in the D Region During an Eclipse," J. Atmos. Terr. Phys. 36 1411-1420 (1974).

3. J. R. Peterson, "Sunlight Photodestruction of CO_3^-, $CO_3^- \cdot H_2O$, and O_3^-: The Importance of Photodissociation to the D Region Electron Densities at Sunrise," J. Geophys. Res. 81, 1433-1435 (1976).

4. L. M. Branscomb, S. J. Smith, and G. Tisone, "Oxygen Metastable Atom Production Through Photodetachment," J. Chem. Phys. 43, 2906-2907 (1965), and references contained therein.

5. S. P. Hong, S. B. Woo, and E. M. Helmy, "Photodetachment of Thermally Relaxed CO_3^-," Phys. Rev. A 15, 1562-1569 (1977), and references contained therein.

6. P. Warneck, "Laboratory Measurements of Photodetachment Cross Sections of Selected Negative Ions," GCA Technical Report 69-13-N, GCA Corporation, Bedford, MA (1969).

7. R. A. Beyer and J. A. Vanderhoff, "Cross Section Measurements for Photodetachment or Photodissociation of Ions Produced in Gaseous Mixtures of O_2, CO_2, and H_2O," J. Chem. Phys. 65, 2313-2321 (1976).

8. L. M. Colonna-Romano, "Microcomputer Automation of the BRL Photodestruction Experiment," BRL Report in preparation.

9. P. C. Cosby, J. H. Ling, J. R. Peterson, and J. T. Moseley, "Photodissociation and Photodetachment of Molecular Negative Ions: III. Ions Formed in $CO_2/O_2/H_2O$ Mixtures," J. Chem. Phys. 65, 5267-5274 (1976).

10. E. W. McDaniel and E. A. Mason, The Mobility and Diffusion of Ions in Gases, p. 291 (Wiley, New York, 1973).

11. S. B. Woo, L. M. Branscomb, and E. C. Beaty, "Sunlight Photodetachment Rate of Ground State O_2^-," J. Geophys. Res. 96, 2933-2940 (1969) and references contained therein.

12. D. S. Burch, S. J. Smith, and L. M. Branscomb, "Photodetachment of O_2^-," Phys. Rev. 112, 171-175 (1958).

REFERENCES (CONTD)

13. P. C. Cosby, G. P. Smith, J. T. Moseley, and L. C. Lee, "Photodissociation of Atmospheric Positive Ions," 30th Annual Gaseous Electronics Conference, MA-6, Oct. 1977.

14. D. L. Albritton, T. M. Miller, D. W. Martin, and E. W. McDaniel, Mobilities of Mass Identified H_3^+ and H^+ Ions in Hydrogen," Phys. Rev. 171, 94-102 (1968).

15. E. Herbst, T. A. Patterson, and W. C. Lineberger, "Laser Photodetachment of NO_2^-," J. Chem. Phys. 61, 1300-1304 (1974).

16. B. A. Huber, P. C. Cosby, J. R. Peterson, and J. T. Moseley, "Photodetachment and De-excitation of Excited NO_2^{-*}," J. Chem. Phys. 66, 4520-4526 (1977).

17. R. J. Celotta, R. A. Bennett, and J. L. Hall, "Laser Photodetachment Determination of the Electron Affinities of OH, NH_2, NH, SO_2, and S_2," J. Chem. Phys. 60, 1470-1745 (1974).

18. D. Feldman, "Photoablösung von Elektronen bei einigen Stabilen Negativen Ionen," Z. Naturforsch 25a, 621-626 (1970).

19. S. F. Wong, T. V. Vorburger, and S. B. Woo," Photodetachment of O_3^- in a Drift Tube," Phys. Rev. A 5, 2598-2604 (1972).

20. J. T. Moseley, P. C. Cosby, and J. R. Peterson, "Photodissociation Spectroscopy of CO_3^-," J. Chem. Phys. 65, 2512-2517 (1976), and references contained therein.

21. M. L. Vestal, "Fundamental Research Relating to New Laser Systems," Final Report on Air Force Contract F33615-73-C-4128, March 1976.

22. G. P. Smith, P. C. Cosby, and J. T. Moseley, "Photodissociation of Atmospheric Positive Ions I. 5300-6700Å," J. Chem. Phys. 67, 3818-3828 (1977).

23. R. R. Burke and R. P. Wayne, "Photodissociation of Positive Cluster Ions by CW and Pulsed Laser Radiation," Int. J. Mass. Spectr. Ion Phys. 25, 199-209 (1977).

24. J. A. Vanderhoff, "Photodissociation of $NO^+(NO)$ and $NO^+(H_2O)$," J. Chem. Phys. 67, 2332-2337 (1977).

25. W. R. Henderson and A. L. Schmeltekopf, "Photolysis of Hydrated Oxonium Ions in the Spectral Range of 5800Å to 6100Å," J. Chem. Phys. 57, 4502-4503 (1972).

26. D. C. Conway and Jae-Hyun Yang, "Bonding in Homonuclear Ion Clusters," J. Chem. Phys. 43, 2900-2902 (1965).

DISTRIBUTION LIST

No. of Copies	Organization
12	Commander Defense Documentation Center ATTN: DDC-TCA Cameron Station Alexandria, VA 22314
1	Director Institute for Defense Analyses ATTN: Dr. E. Bauer 400 Army-Navy Drive Arlington, VA 22202
2	Director Defense Advanced Research Projects Agency ATTN: STO, CPT J. Justice Dr. S. Zakanyca 1400 Wilson Boulevard Arlington, VA 22209
1	Director of Defense Research and Engineering ATTN: CAPT K. W. Ruggles Washington, DC 20305
4	Director Defense Nuclear Agency ATTN: STAP (APTL) STRA (RAAE) Dr. C. Blank Dr. H. Fitz, Jr. DDST Washington, DC 20305
2	DASIAC/DOD Nuclear Information and Analysis Center General Electric Company-TEMPO ATTN: Mr. A. Feryok Mr. W. Knapp 816 State Street P. O. Drawer QQ Santa Barbara, CA 93102
1	Director Defense Communication Agency ATTN: Code 340, Mr. W. Dix Washington, DC 20305
1	Commander US Army Materiel Development and Readiness Command ATTN: DRCDMD-ST 5001 Eisenhower Avenue Alexandria, VA 22333
1	Commander US Army Aviation Research and Development Command ATTN: DRSAV-E P. O. Box 209 St. Louis, MO 63166
1	Director US Army Air Mobility Research and Development Laboratory Ames Research Center Moffett Field, CA 94035
1	Commander US Army Electronics Research and Development Command Technical Support Activity ATTN: DELSD-L Fort Monmouth, NJ 07703
5	Commander/Director Atmospheric Sciences Laboratory ATTN: Dr. F. E. Niles Mr. H. Ballard Dr. E. H. Holt Dr. M. G. Heaps Dr. D. E. Snider White Sands Missile Range NM 88002

DISTRIBUTION LIST

No. of Copies	Organization
1	Commander US Army Communications Rsch and Development Command ATTN: DRDCO-SGS Fort Monmouth, NJ 07703
1	Commander US Army Missile Research and Development Command ATTN: DRDMI-R Redstone Arsenal, AL 35809
1	Commander US Army Missile Materiel Readiness Command ATTN: DRSMI-AOM Redstone Arsenal, AL 35809
1	Commander US Army Tank Automotive Research & Development Cmd ATTN: DRDTA-UL Warren, MI 48090
2	Commander US Army Armament Research and Development Command ATTN: DRDAR-TSS Dover, NJ 07801
1	Commander US Army Armament Materiel Readiness Command ATTN: DRSAR-LEP-L, Tech Lib Rock Island, IL 61299
1	Commander US Army Harry Diamond Labs ATTN: DRXDO-NP, F. Wimenitz 2800 Powder Mill Road Adelphi, MD 20783
1	Director US Army TRADOC Systems Analysis Activity ATTN: ATAA-SL, Tech Lib White Sands Missile Range NM 88002
1	Commander US Army Nuclear Agency ATTN: Mr. J. Berberet 7500 Backlick Rd., Bldg 2073 Springfield, VA 22150
1	Commander US Army Research Office ATTN: Dr. R. Lontz P. O. Box 12211 Research Triangle Park NC 27709
1	HQDA (DAEN-RDM, Dr. de Percin) Washington, DC 20314
1	Chief of Naval Research ATTN: Code 418, Dr. J. Dardis Department of the Navy Washington, DC 20360
1	Commander Naval Surface Weapons Center ATTN: Dr. L. Rutland Silver Spring, MD 20910
1	Commander Naval Electronics Laboratory ATTN: Mr. W. Moler San Diego, CA 92152
3	Commander Naval Research Laboratory ATTN: Dr. W. Ali Code 7700, Mr. J. Brown Code 2020, Tech Lib Washington, DC 20375

DISTRIBUTION LIST

No. of Copies	Organization
3	HQ USAF (AFNIN; AFRD; AFRDQ) Washington, DC 20330
2	AFSC (DLCAW, LTC R. Linkous; SCS) Andrews AFB Washington, DC 20334
7	AFGL (LKD, Dr. R. Narcisi LKB, Dr. K. Champion, Dr. T. Keneshea, Dr. J. Paulson, Dr. W. Swider OPR, Dr. Murphey, Dr. Kennelly Hanscon AFB, MA 01730
1	Director National Oceanic and Atmospheric Administration ATTN: Dr. E. Ferguson US Department of Commerce Boulder, CO 80302
1	Director Brookhaven National Laboratory ATTN: Docu Sec 25 Brookhaven Avenue Upton, NY 11973
2	Director Los Alamos Scientific Lab ATTN: Lib Dr. W. Maier (Gp J-10) P. O. Box 1663 Los Alamos, NM 87544
1	Director Jet Propulsion Laboratory ATTN: Dr. W. Huntress 4800 Oak Grove Drive Pasadena, CA 91103
1	Bell Telephone Labs, Inc. Technical Report Service ATTN: Tech Rpts Specialist Whippany, NJ 07981
1	General Electric Company Valley Forge Space Technology Center ATTN: Dr. M. Bortner P. O. Box 8555 Philadelphia, PA 19101
1	Mission Research Corporation ATTN: Dr. M. Scheibe 735 State Street P. O. Drawer 719 Santa Barbara, CA 93102
1	R&D Associates ATTN: Dr. F. Gilmore P. O. Box 9695 Marina del Rey, CA 90291
2	Sandia Laboratories ATTN: Org 3141, Tech Lib Ord 100, F. Hudson Albuquerque, NM 87115
1	Georgia Institute of Tech School of Physics ATTN: I. R. Gatland Atlanta, GA 30332
1	Pennsylvania State University Ionospheric Research Lab ATTN: Dr. L. C. Hale University Park, PA 16802
4	Stanford Research Institute ATTN: Dr. J. Peterson Dr. J. Moseley Dr. P. Cosby Dr. F. Smith 333 Ravenswood Avenue Menlo Park, CA 94025

DISTRIBUTION LIST

No. of Copies Organization

1 State University of New York
Dept of Atmospheric Sciences
ATTN: Dr. V. Mohnen
Albany, NY 12203

1 CIRES
University of Colorado
ATTN: Dr. A. W. Castleman
Boulder, CO 80302

2 University of Colorado
Joint Institute for Laboratory Astrophysics
ATTN: Dr. W. C. Lineberger
Dr. A. V. Phelps
Boulder, CO 80304

1 University of Delaware
Department of Physics
ATTN: Prof. S. B. Woo
Newark, DE 19711

1 University of Denver
Denver Research Institute
ATTN: Dr. R. Amme
P. O. Box 10127
Denver, CO 82010

1 University of Illinois
Electrical Engineering Dept
Aeronomy Laboratory
ATTN: Prof. C. Sechrist
Urbana, IL 61801

1 University of Minnesota, Morris
Div of Science & Mathematics
ATTN: Dr. M. N. Hirsh
Morris, MN 56267

No. of Copies Organization

1 University of Missouri-Rolla
Department of Physics
ATTN: Dr. R. Anderson
105 Physics Building
Rolla, MO 65401

1 University of Pittsburgh
Cathedral of Learning
ATTN: Dr. M. A. Biondi
400 Bellefield Avenue
Pittsburgh, PA 15213

1 University of Utah
Chemistry Department
ATTN: Dr. M. L. Vestal
Salt Lake City, UT 84112

Aberdeen Proving Ground

Dir, USAMSAA
Cdr, USATECOM
ATTN: DRSTE-SG-H